

Spatial distribution of ground shaking

D.J. Dowrick & D.A. Rhoades

Institute of Geological & Nuclear Sciences, Lower Hutt.



2005 NZSEE
Conference

ABSTRACT: In empirical models of attenuation of strong motion, peak ground acceleration and spectral acceleration (PGA and SA), source-to-site distances are usually defined as the shortest distance from the site to a planar region, representing the fault rupture. Such a definition constrains the attenuation model to have racetrack-shaped lines of equal PGA or SA. It can result in errors (i.e., deviations of the fitted model from the data) which are substantial in the near-source region. This is demonstrated by comparison with the attenuation models that arise when no such constraints are built into the source-to-site distances, as is the case in the Dowrick and Rhoades attenuation model for Modified Mercalli intensity (MMI). The nature and magnitude of the errors in the strong-motion attenuation models are described for a magnitude 7.5 earthquake.

1 INTRODUCTION

The modelled spatial distribution of earthquake ground shaking, or its effects, vary widely depending on a number of factors, notably:

- The ground shaking measure, e.g. PGA, SA or MMI
- The assumed geometry of the source
- The adopted definition of the source-to-site distance
- The form of the attenuation function.

The most common modelled patterns of spatial distribution are shown in Figure 1. For predictive modelling of the attenuation of ground motions, it has long been common practice to use distances that are measured as the shortest distance, r , from source-to-site (e.g. Abrahamson and Silva 1997). This results in iso-strong-motion (isoSM) lines of race track shape, Figure 1(a), or the more complicated shape of Figure 1(b), depending on whether the fault rupture is vertical or not. The shortest distance assumption results in the isoSM lines always enclosing the vertical projection of the top of the assumed subsurface rupture, length L_{sub} in Figure 1(a).

An alternative to measuring distances from individual observation sites to an areal source, is to measure the dimensions in two orthogonal directions of isoSMs or isoseismals. This method has been used for isoseismals by Dowrick & Rhoades (1999), the axes (a and b) for measuring being along and normal to the fault strike (Fig. 2). Using this approach, the modelled iso-lines are elliptical in shape (Fig. 1(c)), reflecting the “true” idealized shapes of the mean isoseismals while the length of the modelled isoseismals need not exceed L_{sub} . These remarks are well supported by the distribution of the local observations. An example of this is given by the M_w 7.8 1931 Hawke’s Bay earthquake (Fig. 3), where it is seen that the MM10 isoseismal has a length of $2a = 40$ km, whereas the rupture length is $L_{sub} = 90$ km. This is reflected in the attenuation modelling of Dowrick & Rhoades (1999; in prep., 1),

as seen on Figure 4 for a strike-slip earthquake of M_W 7.8. The rupture length estimate comes from Dowrick & Rhoades (2004).

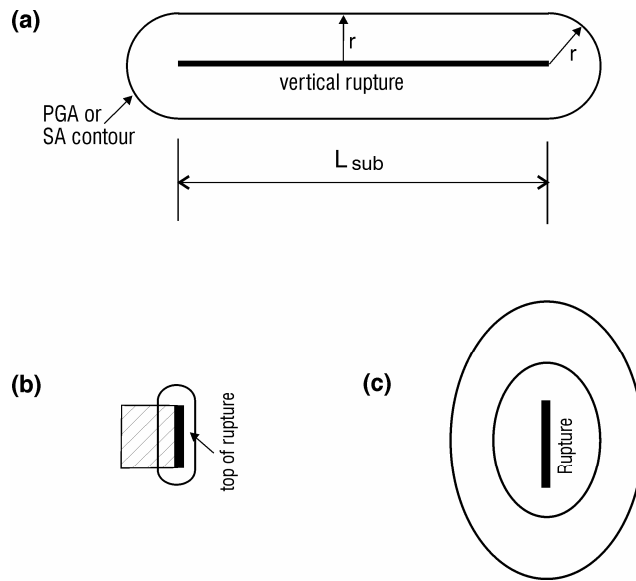


Figure 1 Examples of modelled spatial patterns of ground motions: (a) shortest distance to vertical planar source, (b) shortest distance to non-vertical planar source and (c) elliptical model.

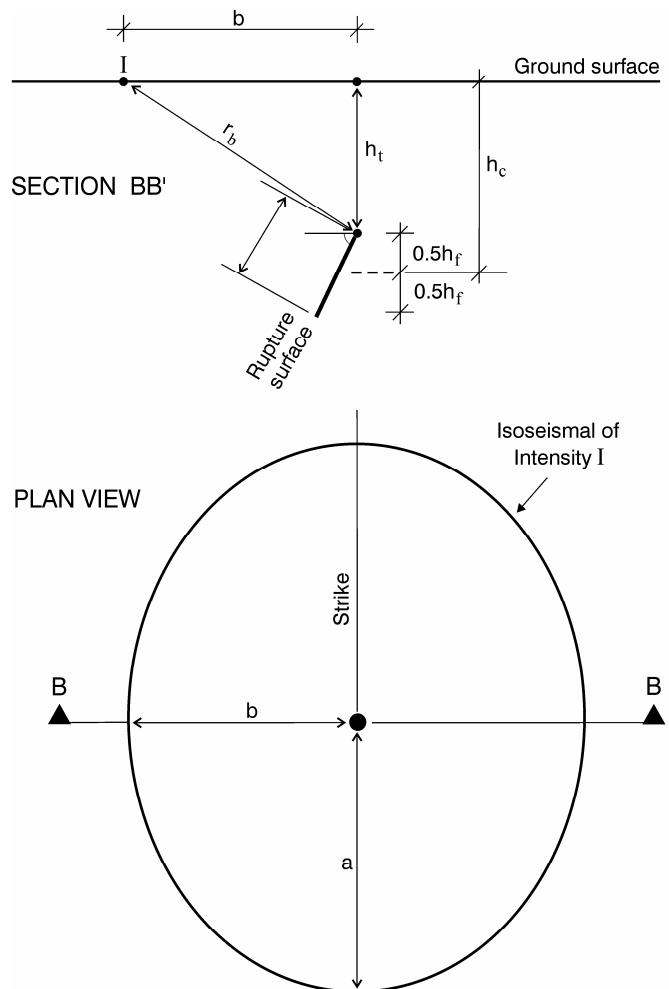


Figure 2 Elliptical pattern of isoseismals resulting from deriving separate attenuation models for the along-strike direction (dimension a) and strike-normal direction (dimension b) (after Dowrick & Rhoades 1999).

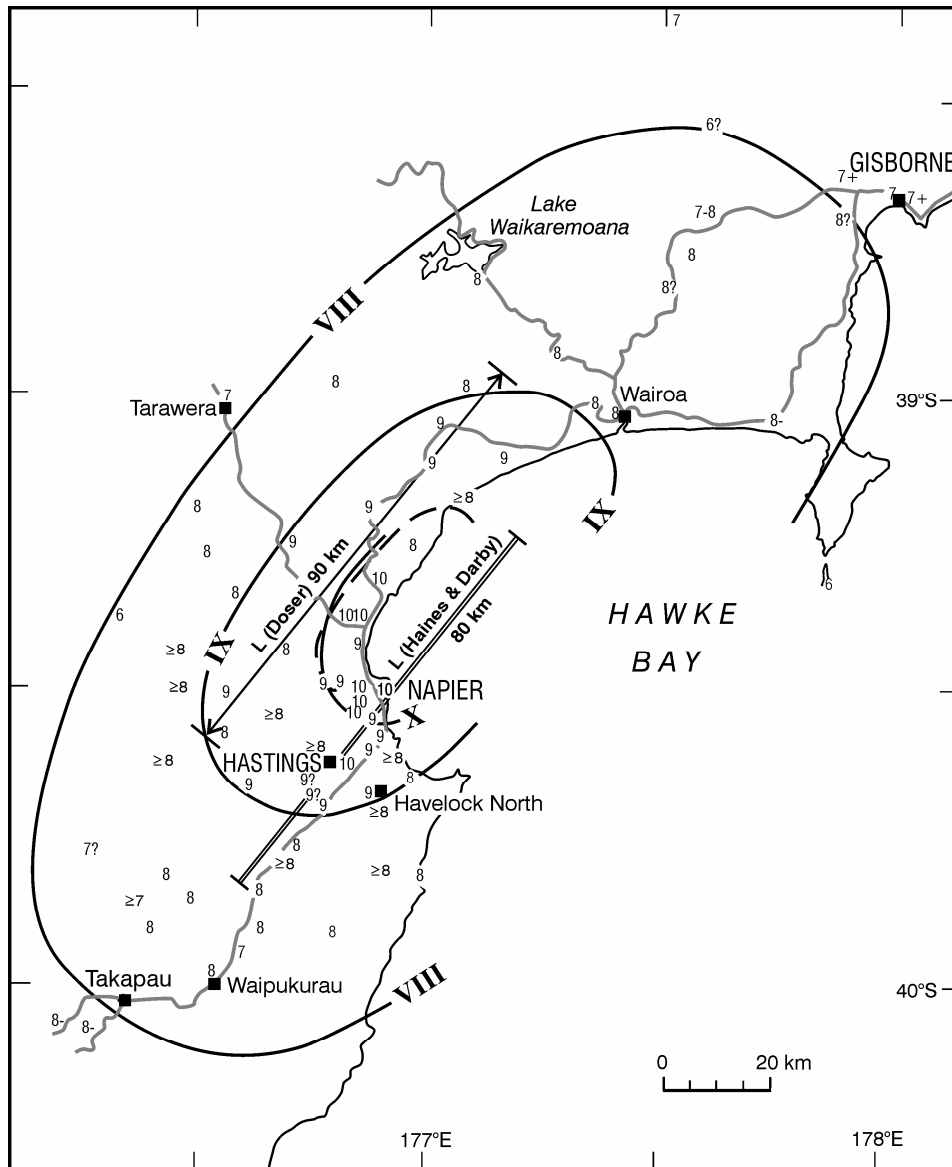


Figure 3 Map of the M_w 7.8 Hawke's Bay earthquake of 1931, showing the length of the adopted rupture ("L (Doser)" from Dowrick & Rhoades, 2004), the top of the rupture modelled by Haines & Darby (1987), and the inner isoseismals (from Dowrick 1998).

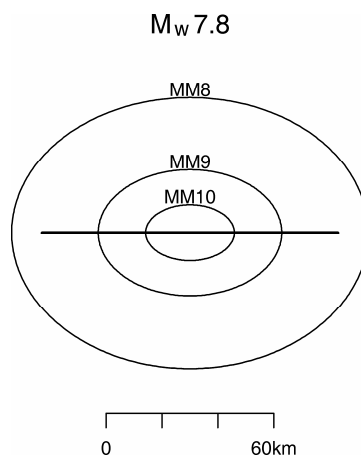


Figure 4 Plot of modelled inner isoseismals and fault rupture length for a surface rupturing strike-slip New Zealand earthquake of M_w 7.8.

Our aim is to highlight some important discrepancies between the elliptical and racetrack models. To do this we (i) create a set of data points using an elliptical model, (ii) fit a racetrack attenuation model to the “elliptical” data, and (iii) compare various predictions derived from the two models.

2 REGRESSIONS OF ELLIPTICAL DATA USING SHORTEST SOURCE-TO-SITE DISTANCE

On Figure 5 are shown the elliptical isoseismals for a surface rupturing strike-slip earthquake of M_w 7.5, as predicted by the attenuation model of Dowrick & Rhoades (in prep., 1), which has the functional form

$$I = a_1 + a_2 \log D + a_3 M_w + a_4 h_c \quad (1)$$

where distance

$$D = (r^3 + d^3)^{1/3} \quad (2)$$

Parameter r is the distance to the top of the centre of the rupture surface (Figure 2), h_c is the centroid depth source constraint, and d is a fitted parameter which provides near-source constraint.

For our regression analyses we use 40 ground shaking data points located randomly within the area enclosed by the MM4 isoseismal shown on Figure 5, and assign to each data point the intensity predicted by the model of Dowrick & Rhoades (in prep., 1). In the following analyses we work in terms of the peak ground accelerations (PGA) equivalent to the Modified Mercalli (MM) isoseismals (I) and estimate it from a speculative non-linear curve, which is deemed to be adequate for the present purposes:

$$\log \text{PGA} = -4.870 + 0.884I - 0.0381I^2 \quad (3)$$

where PGA is in g. This quadratic curve is fitted to closely approximate the log-linear expression of Davenport (2003) derived from New Zealand data:

$$\log \text{PGA} = -3.69 + 0.426 I \quad (4)$$

for intensities MM4-MM7, and also the value $\text{PGA} = 0.65\text{g}$ at the MM10 isoseismal, which conforms approximately with near-source strong motion values.

Having regard to equations (1) and (2), the relation

$$\log \text{PGA} = a_1 + a_2 \log D \quad (5)$$

is then fitted to the data for a given value of magnitude (m), with D as in equation (2), except that r now represents the shortest source-site distance as shown on Figure 1(a). The relation has three fitted parameters: a_1 , a_2 and d . However, the fit of equation (5) was constrained so that

$$a_1 + a_2 \log d = \max \text{PGA} \quad (6)$$

where $\max \text{PGA}$ is the PGA value corresponding, according to equation (3), to the maximum MM intensity predicted for an earthquake of magnitude m by the model of Dowrick & Rhoades (in prep.,

1). This constraint ensures that the fitted PGA has the same maximum as in the original model.

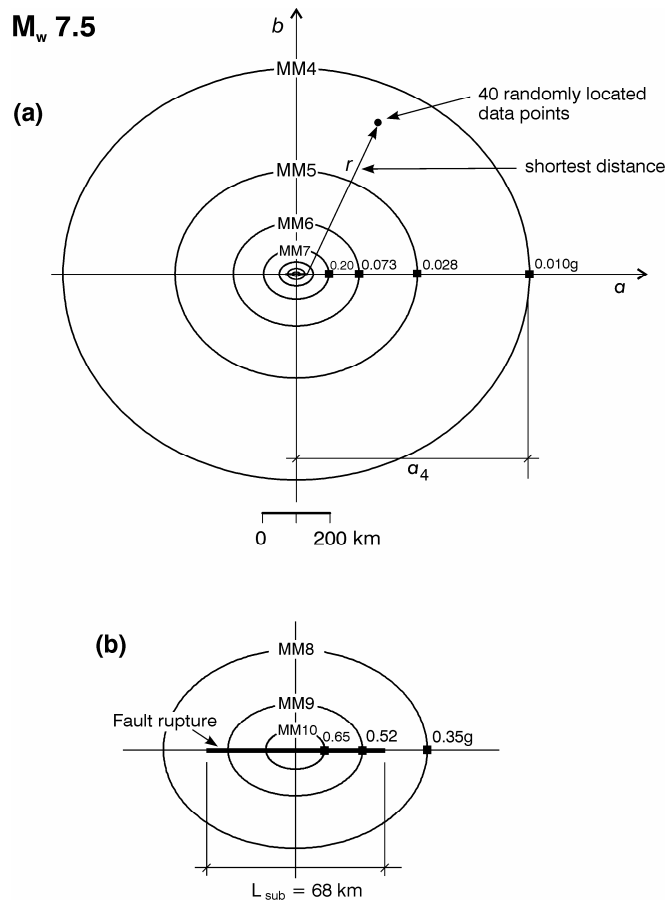


Figure 5 Data map for Case 1, representing the idealized elliptical spatial distribution of intensities and PGAs of a magnitude 7.5 New Zealand earthquake, with rupture length $L_{sub} = 68$ km, (a) outer isoseismals, and (b) detail of inner isoseismals. Case 2 is the same as this except that the fault rupture is aligned at 90 degrees to the major axis of the ellipses.

3 RACETRACK AND ELLIPTICAL AREAS INSIDE ISOPGAS

The areas inside the racetrack isoPGAs (A_r) and the elliptical isoPGAs (A_e) are plotted on Figure 6 as functions of PGA, for a strike-slip New Zealand earthquake of M_w 7.5 (Figure 5). It is seen that the areas given by the two models are approximately equal in the far field, ie. for $A(\text{isoPGA}) > c. 27,000$ km² and for $\text{PGA} < c. 0.17g$, while for stronger shaking A_r becomes progressively larger than A_e such that at $\text{PGA} = 0.65g$:

$$A_r = 6.8A_e \quad (7)$$

4 RACETRACK AND ELLIPTICAL ISOPGA SPATIAL PATTERNS

We now consider the spatial patterns arising from racetrack models derived from two very different spatial distributions of data, ie Case 1 as shown on Figure 5 and Case 2 (which is the same as Case 1 except that the rupture is rotated through 90 degrees). Thus, Case 2 is unrealistic, but is used to make a point. The spatial patterns for these two cases are plotted on Figure 7, which shows that the models for the two very different data distributions are very similar. This results directly from the use of the shortest source-to site distance.

The values of PGA at any given site, as predicted by the racetrack and elliptical models, are compared

by the value of the ratio

$$R_{r/e} = \text{PGA}_r / \text{PGA}_e \quad (8)$$

These values have been plotted spatially on Figure 8 for Case1 (Fig. 5). It is seen that $R_{a/e}$ ranges up as high as 1.8 in zones within c.20 km of the ends of the rupture, to as little as less than 0.9 about 80 km along a line normal to the centre of the rupture.

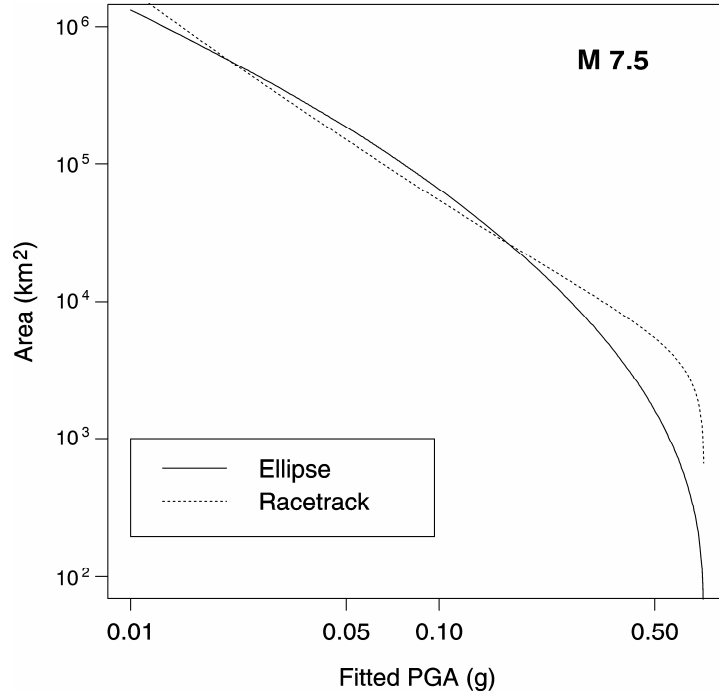


Figure 6 Plots of area inside the isoPGA lines for the racetrack and elliptical models for a strike-slip New Zealand earthquake of M_w 7.5.

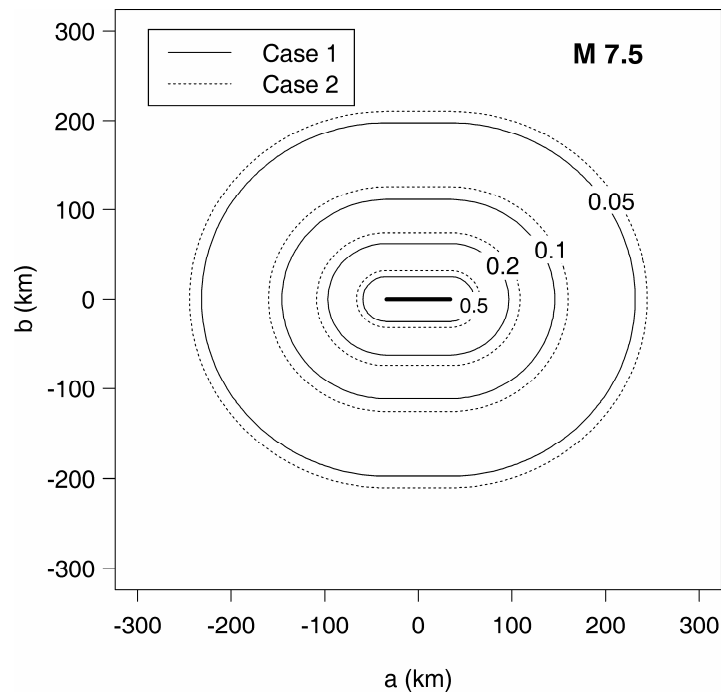


Figure 7 Comparison of isoPGA patterns using the racetrack models of the very different spatial distributions of data of Cases 1 and 2 (Figure 5).

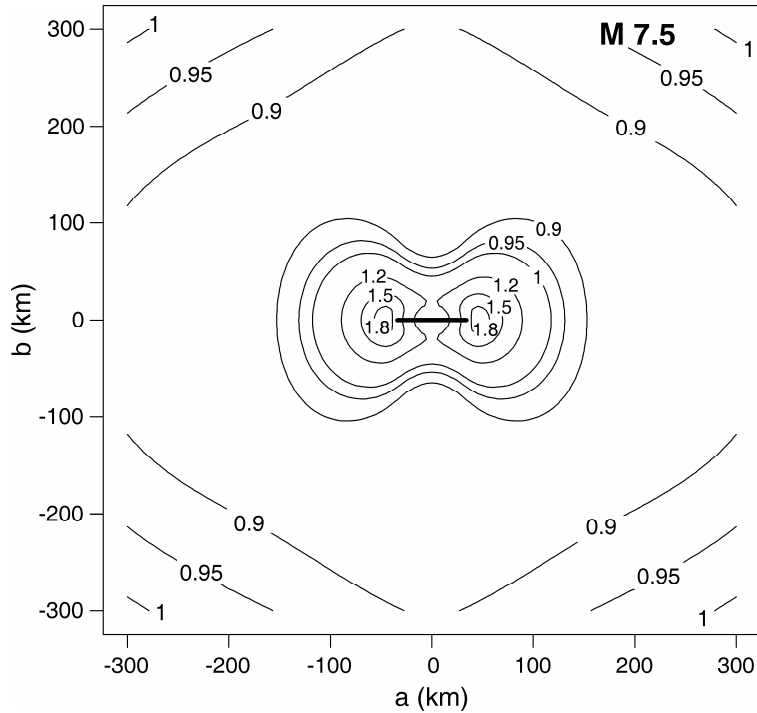


Figure 8 Spatial plot of the ratio PGA_r/PGA_e for a strike-slip New Zealand earthquake of $M_w 7.5$, with $L_{sub} = 68$ km.

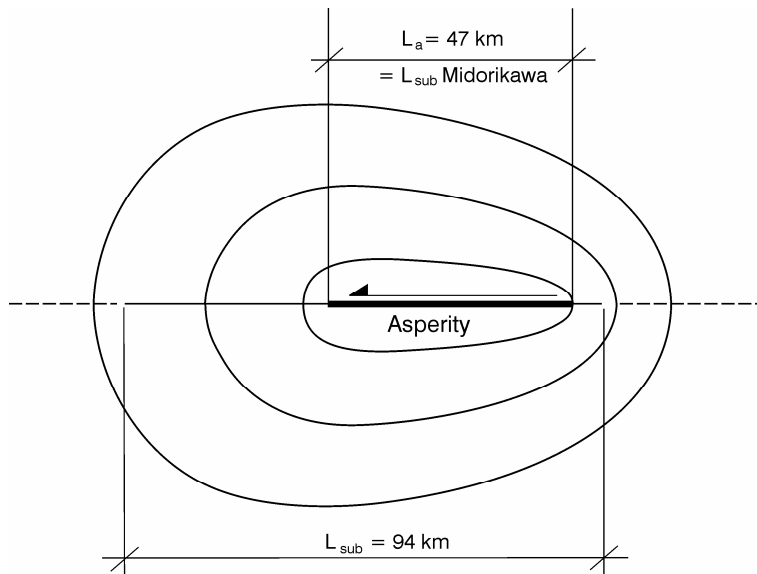


Figure 9 Spatial plot of isoPGA lines considering Midorikawa's rupture length of 47 km to be the (only) asperity on the rupture surface with $L_{sub} = 94$ km.

5 ASPERITIES

The near-source spatial distribution of ground shaking is no doubt largely controlled by the nature and distribution of asperities on the rupture surface, as the asperities localize the areas from which earthquakes waves are generated. For example in Californian earthquakes the area of the asperities, A_a , averages about twenty percent of the rupture surface, A (Somerville *et al*, 1999). For New Zealand the mean value of A_a/A is not yet known, but is not more than 50 percent (Dowrick & Rhoades in prep. 2).

A simple demonstration of the effect of asperities is made by considering the spatial distribution

pattern of Midorikawa (1993), as shown on Figure 9. Midorikawa calculated the spatial distribution of PGAs on the assumption that the strain energy release was uniformly distributed across the whole rupture surface, with $L_{\text{sub}} = 47$ km (Fig. 9). In the figure we assume that Midorikawa's rupture surface is the asperity on a larger surface with $L_{\text{sub}} = 94$ km. From Figure 9 it is seen that the innermost isoPGA line is much shorter than the full length of the rupture, in keeping with Figure 3 and the findings for MMIs and PGAs when no constraints are placed on source-to-site distances.

6 CONCLUSIONS

1. The use of the shortest source-to-site distance in strong ground motion attenuation models may lead to substantial errors in the prediction of spatial distribution of ground motions in the near-source area.
2. For a strike slip New Zealand earthquake of M_w 7.5, the area inside the racetrack model of the iso-line for $\text{PGA} = 0.65g$ is 6.8 times greater than that for an elliptical model.
3. A racetrack attenuation model constrains the spatial patterns of PGA to be very similar, regardless of the spatial distribution of the local observations.
4. For a strike-slip New Zealand earthquake of M_w 7.5, the spatial pattern of the ratio $\text{PGA}_r/\text{PGA}_e$ shows that the racetrack model over-estimates the elliptical PGA by up to 1.8 times in the zones within c. 20 km of the ends of the rupture.
5. Attenuation models for strong motion parameters need to be based on a more realistic distance term than that which is currently used.

ACKNOWLEDGEMENTS

This study was funded by the New Zealand Foundation for Research Science and Technology under Contract No. CO5X0402. We thank Jim Cousins and Peter Davenport for their in-house reviews.

REFERENCES:

- Abrahamson, N. & Silva, W. 1997. Empirical response attenuation relations for shallow crustal earthquakes. *Seism. Res. Letters* 68(1). 94-117.
- Davenport, P.N. 2003. Instrumental measures of earthquake intensity in New Zealand. *Proc. Pacific Conf. on Earthq. Eng.* Christchurch. Paper 071 (published on CD-rom).
- Dowrick, D.J. 1998. Damage and intensities in the magnitude 7.8 1931 Hawke's Bay, New Zealand, earthquake. *Bull. N. Z. Nat. Soc. Earthq. Eng.* 31(3). 139-163.
- Dowrick, D. J. & Rhoades, D.A. 1999. Attenuation of Modified Mercalli intensity in New Zealand earthquakes. *Bull. N. Z. Nat. Soc. Earthq. Eng.* 32(2). 55-89.
- Dowrick, D.J. & Rhoades, D.A. 2004. Relations between earthquake magnitude and fault rupture dimensions: How regionally variable are they? *Bull. Seism. Soc. Amer.* 94(3). 776-788.
- Dowrick, D.J. & Rhoades, D.A. in prep. 1. Attenuation of Modified Mercalli intensity in New Zealand earthquakes (II).
- Dowrick, D.J. & Rhoades, D.A. in prep. 2. Why relations between earthquake magnitude and fault rupture dimensions vary regionally.
- Haines, A.J. & Darby, D.J. 1987. Preliminary dislocation models for the 1931 Napier and 1932 Wairoa earthquakes. *N. Z. Geol. Surv. Report EDS 114*.
- Midorikawa, S. 1993. Semi-empirical estimation of peak ground acceleration from large earthquakes. *Tectonophysics* 218. 287-295.
- Somerville, P., Irakura, K., Graves, R., Sawada, S., Wald, D., Abrahamson, N., Iwasaki, Y., Kagawa, T. & Smith, N. 1999. Characterizing crustal earthquake slip models for the prediction of strong ground motion. *Seism. Res. Letters* 70(1). 59-80.